Author Manuscript

Author Manuscript

Author Manuscript

Author Manuscript

HHS Public Access

Author manuscript

*Nat Med*. Author manuscript; available in PMC 2018 July 15.

Published in final edited form as:

*Nat Med*. 2018 February ; 24(2): 224–231. doi:10.1038/nm.4467.

# Transitory presence of myeloid-derived suppressor cells in neonates is critical for control of inflammation

**Yu-Mei He**[*,1,3], **Xing Li**[*,1,3,4], **Michela Perego**[*,2], **Yulia Nefedova**[2], **Andrew V. Kossenkov**[2], **Erik A. Jensen**[5], **Valerian Kagan**[6], **Yu-Feng Liu**[1], **Shu-Yu Fu**[1], **Qing-Jian Ye**[4], **Yan-Hong Zhou**[7], **Lai Wei**[8], **Dmitry I. Gabrilovich**[1,2,3,#], and **Jie Zhou**[1,3,7,#]

[1]Institute of Human Virology, Zhongshan School of Medicine, Sun Yat-sen University, Guangzhou, China

[2]The Wistar Institute, Philadelphia, PA, USA, 19104

[3]Key Laboratory of Tropical Disease Control, Chinese Ministry of Education, Guangzhou, China

[4]The Third Affiliated Hospital, Sun Yat-sen University

[5]The Children's Hospital of Philadelphia, Philadelphia, PA, USA, 19104

[6]Department of Environmental and Occupational Health, University of Pittsburgh, PA, 15219

[7]Guangzhou Women and Children's Medical Center, Guangzhou

[8]Zhongshan Ophthalmic Center, Sun Yat-sen University

## Abstract

Myeloid-derived suppressor cells (MDSC) are pathologically activated and relatively immature myeloid cells, which are implicated in the immune regulation of many pathologic conditions[1,2]. Phenotypically and morphologically MDSC are similar to neutrophils (PMN-MDSC) and monocytes (M-MDSC). However, they have potent suppressive activity, a distinct gene expression profile, and biochemical characteristics[3]. None or very few MDSC are observed in steady state physiological conditions. Therefore, until recently, accumulation of MDSC was considered as a consequence of pathological process or pregnancy. Here, we report that MDSC with a potent ability to suppress T cells are present during the first weeks of life in mice and humans. MDSC suppressive activity was triggered by lactoferrin and mediated by nitric oxide, PGE2, and S100A9/A8 proteins. Newborn MDSC had a transcriptome similar to that of tumor MDSC, but with a strong up-regulation of an antimicrobial gene network and had potent antibacterial activity.

Users may view, print, copy, and download text and data-mine the content in such documents, for the purposes of academic research, subject always to the full Conditions of use: http://www.nature.com/authors/editorial_policies/license.html#terms

Correspondence: Dmitry I Gabrilovich (dgabrilovich@wistar.org) or Jie Zhou (zhouj72@mail.sysu.edu.cn).
*These authors contribute equally to this work
#Shared senior authorship

**Conflict of Financial Interests**

Authors declare no financial conflicts.

**Authors contributions**

Conceptualization, D.I.G. J.Z., Formal Analysis A.V.K., Investigation, Y.-M.H., X.L., M.P., Y.-F.L., S.-Y.F., Q.-J.Y., Y.-H.Z., L.W. Resources, Y.N., E.A.J., Writing – original draft – D.I.G., J.Z., Writing – Review & Editing, D.I.G., J.Z., Y.N., V.K. Supervision, D.I.G., J.Z., Funding Acquisition, D.I.G., J.Z.,V.K.

Author Manuscript Author Manuscript Author Manuscript Author Manuscript

MDSC played a critical role in control of experimental necrotizing enterocolitis (NEC) in newborn mice. MDSC in infants with very low-weight, which are prone to the development of NEC, had lower MDSC levels and suppressive activity than infants with normal weight. Thus, the transitory presence of MDSC may be critical for regulation of inflammation in newborns.

---

Although MDSC are largely absent in healthy adults, recent evidence indicates that MDSCs may play a role in the maintenance of maternal-fetal tolerance[4]. The role of MDSC in pregnancy would be consistent with a myeloid cell response to partial genetic incomparability between mother and child. In this study, we tested the possible role of MDSC in steady state conditions during first weeks of life.

Populations of myeloid cells were evaluated in spleens and bone marrow (BM) of adult mice (6–8 weeks of age) (AM), newborn mice (NBM), and in mice within 7 days after giving birth (postpartum mice, PM). In comparison to AM and PM, 7–10 days old NBM had substantial increase in splenic $CD11b^{+}Ly6C^{hi}Ly6G^{-}$ monocytes and $CD11b^{+}Ly6C^{lo}Ly6G^{+}$ neutrophils (Supplementary Fig. 1a). Cells from NBM and AM had similar morphology (Supplementary Fig. 1b). The proportion of these populations was the highest on day 1 after birth and gradually decreased by the end of week 2 when it reached the levels observed in AM (Fig. 1a). The population of spleen macrophages was not different, whereas dendritic cells were decreased (Supplementary Fig. 1c). In contrast to AM, monocytes from 7–10 days old NBM potently inhibited proliferation of $CD4^{+}$ and $CD8^{+}$T cells (Fig. 1b) and neutrophils demonstrated potent suppression of antigen-specific proliferation of $CD8^{+}$ T cells (Fig. 1c). Thus, these cells fit the criteria of M-MDSC and PMN-MDSC, respectively[3]. In NBM, MDSC suppressive activity was not observed during first 3 days and disappeared after day 14 (Fig. 1d,e). Spleen macrophages did not have suppressive activity (Supplementary Fig. 1d). In lactating PM, the number of monocytes and neutrophils did not differ from that in AM and no suppressive activity was detected (Supplementary Fig. 1e–h). Thus, MDSC were found exclusively in NBM.

To assess the ability of NBM MDSC to control autoimmune inflammation, AM were sensitized and challenged with intranasal administration of OVA (Supplementary Fig. 2a). Administration of NBM MDSC, but not AM neutrophils, reduced lung inflammation (Supplementary Fig. 2b,c), the presence of leukocytes, the amount of IL-13 and IL-4 in bronchoalveolar lavage (Supplementary Fig. 2d–g), and IgE in sera (Supplementary Fig. 2h).

$CD11b^{+}Ly6C^{lo}Ly6G^{+}$ and $CD11b^{+}Ly6C^{hi}Ly6G^{-}$ cells from spleens of AM and 7 days old NBM were sorted and whole transcriptome analysis was performed using RNA-seq (Supplementary Fig. 3a). Ingenuity Pathway Analysis (IPA) revealed up-regulation of 55 key transcriptional regulators in NBM including lactoferrin (*ltf*), *s100a8,* and *s100a9*. Prostaglandin E synthase *(ptges)* was upregulated in PMN-MDSC. Ptges controls PGE2 synthesis, which is implicated in MDSC function[5,6] (Supplementary Fig. 3b). In previous study, we evaluated the transcriptional profile of MDSCs in tumor-bearing mice[7]. Gene expression profile in NBM MDSC did not correlate with neutrophils and monocytes from tumor free mice but showed correlations with cells from tumor-bearing mice (Supplementary Fig. 3c). Notably, antimicrobial response was the most prominent network found by IPA in NBM MDSC (Supplementary Fig. 3d). NBM PMN-MDSC had more

Author Manuscript Author Manuscript Author Manuscript Author Manuscript

killing of *E. coli* and *C. albicans* than AM neutrophils and NBM M-MDSC were more potent in killing of *E.coli* than AM monocytes (Supplementary Fig. 4a,b).

Our experiments determined that NBM M-MDSC and PMN-MDSC utilized different mechanisms of immune suppression. Up-regulation of *nos2* and NO was responsible for M-MDSC suppression (Supplementary Fig. 5a,b), whereas up-regulation of S100A8/A9 was responsible for NBM PMN-MDSC suppression (Fig. 1f–h). In the absence of these proteins in S100A9KO mice[8] NBM neutrophils lacked suppressive activity, whereas NBM M-MDSC retained it (Fig. 1h). Although association of S100A9/A8 with MDSC is well-known, the specific mechanisms by which these proteins may affect suppressive activity of MDSC were not clear. Based on gene profiling data we focused on Ptges, which is required for terminal PGE2 synthesis[9]. Up-regulation of *ptges* in NBM PMN-MDSC was abrogated in S100A9KO mice (Fig. 1i) suggesting that S100A9 could regulate Ptges. NBM PMN-MDSC from 7-day old mice, but not from 3-day old mice produced a substantially higher amount of PGE2 than neutrophils from AM. Notably, NBM PMN-MDSC from S100A9KO had a similar low amount of PGE2 as AM neutrophils (Fig. 1j) indicating that S100A9/A8 is involved in PGE2 synthesis via regulation of Ptges. In NBM PMN-MDSC and AM neutrophils expression of *cox-2* was similar (Supplementary Fig. 5c). NBM PMN-MDSC from Cox-2KO mice lacking PGE2 production (Supplementary Fig. 5d) had substantially reduced ability to suppress antigen-specific T-cell proliferation (Fig. 1k). Thus, PMN-MDSC activity in NBM was regulated by S100A9/A8 mediated up-regulation of *ptges* and PGE2 production.

The fact that immune suppressive MDSC were detected in NBM between days 4 and 14 might suggest the role of microbial colonization of the gut, which takes place during this period[10]. However, treatment of pregnant mice with combination of antibiotics that depleted gut microbiota (Supplementary Fig. 6a,b) did not affect the presence or suppressive activity of MDSC (Supplementary Fig. 6c–e).

We hypothesized that accumulation of MDSC in NBM could be linked with the milk feeding. It is known that lactoferrin (LF), a component of milk has potent immunoregulatory activity[11]. We tested the effect of LF on myeloid cells *in vivo* by treating 3-week old mice with daily i.p. administration of LF. 8-day treatment caused increase in suppressive MDSC (Fig. 2a–c). Treatment of 6-week old mice with LF did not induce suppressive MDSC suggesting that myeloid progenitors have different susceptibility to LF at different age of the mice. In M-MDSC, LF mediated suppression via *nos2* and NO (Fig. 2d,e), whereas in PMN-MDSC via up-regulation of *s100a8* and *s100a9* (Fig. 2f,g) and PGE2 (Fig. 2h). Treatment of S100A9KO mice with LF did not induce immune suppressive PMN-MDSC (Fig. 2i). In the absence of LF in LFKO mice, granulocytes had no suppressive activity (Fig. 2j), lower S100A9 protein (Fig. 2k) and *ptges* (Fig. 2l) expression, as well as the amount of PGE2 (Fig. 2m) than PMN-MDSC from WT NBM. Taken together, these data indicate that LF may be one of the major factors causing acquisition of immune suppressive activity by MDSC in NBM.

Since myeloid cells can produce LF (Supplementary Fig. 7a), it raises the question about the source of LF that drives accumulation of MDSC. To address this question, we performed

Author Manuscript Author Manuscript Author Manuscript Author Manuscript

cross-fostering experiment. Cross-fostering of WT mice with LFKO surrogates did not result in generation of immune suppressive PMN-MDSC. In contrast, cross-fostering of LFKO NBM with WT mice generated immune suppressive PMN-MDSC (Supplementary Fig. 7b). No differences in the total number of $CD11b^{+}Ly6C^{lo}Ly6G^{+}$ cells were found (Supplementary Fig. 7c). These results indicated a role of LF in the mother's milk in generation of MDSC.

We hypothesized that MDSC may be important for the control of inflammation associated with early microbial colonization in neonates. One of the manifestations of pathological inflammation in neonates is necrotizing enterocolitis (NEC), which is characterized by acute intestinal injury with an associated systemic inflammatory response that may result from the establishment of the gut microbiota[12]. NEC develops in 7–11% of infants born less than 1,500g, termed very low weight (VLW). The estimated mortality rate due to NEC is nearly 30% and approaches 100% among those with the most severe form, NEC *totalis.* It was suggested that abnormalities in immune responses play a critical role in the development of NEC[13]. We investigated changes in MDSC from peripheral blood of newborn infants, between healthy babies with normal weight (NW) (>2,500g) and neonates with VLW (<1,500g). In peripheral blood mononuclear cells (PBMC), healthy adults had very few cells with the phenotype and morphology of PMN-MDSC ($CD11b^{+}CD14^{-}CD15^{+}$) or M-MDSC ($CD11b^{+}CD14^{+}HLA\text{-}DR^{-/lo}CD15^{-}$) (Fig. 3a, Supplementary Fig. 8). Frequencies of MDSC in NW infants were substantially higher than in adults and VLW babies (Fig. 3a). MDSC from NW infants had more potent suppressive activity than cells from VLW babies (Fig. 3b). To verify these findings, we evaluated the presence of $LOX\text{-}1^{+}$ neutrophils in infants. In cancer patients $LOX\text{-}1^{+}CD15^{+}$ neutrophils represented population of PMN-MDSC[14]. Only $LOX\text{-}1^{+}$ but not $LOX\text{-}1^{-}$ neutrophils from NW infants suppressed T-cell function (Fig. 3c). In infants the proportion of $LOX\text{-}1^{+}$ PMN-MDSC was much higher than in adults (Fig. 3d) and frequency of these cells was lower in VLW than in NW infants (Fig. 3e). Only inhibitors of NOS2 – LNMA cancelled suppressive activity of M-MDSC (Fig. 3f). M-MDSC from NW infants but not from VLW infants had increased expression of *NOS2* (Fig. 3g) and the amounts of produced nitrites (Fig. 3h) compared to adult monocytes. PMN-MDSC from NW infants had markedly higher production of PGE2 (Fig. 3i), expression of *S100A9* (Fig. 3j), S100A9 protein (Fig. 3k), and expression of *LTF* (Fig. 3l) than the cells from adults and VLW infants. MDSC from NW and VLW neonates had higher antibacterial activity than neutrophils and monocytes from adults (Supplementary Fig. 9). NW infants who were fed with breast milk had higher level of $LOX\text{-}1^{+}$ PMN-MDSC than infants that received formula lacking LF (Fig. 3m).

We next asked whether MDSC are important in NEC. We used a gavage/hypoxia experimental model of NEC[15], which manifests as inflammatory gut injury of varied intensity (Fig. 4a). Although this model, as any other model of NEC, cannot fully recapitulate human disease, it generates conditions (intestinal necrosis and inflammation) that are similar to those observed in humans. Induction of NEC in 1-day old NBM (with no MDSC present) caused much more severe inflammation compared to 4-day old NBM (with MDSC present), which manifested in higher intestine permeability (Fig. 4b), inflammation scores (Fig. 4c) and shorter survival (Fig. 4d). The differences in bacterial load were small but significant ($p=0.018$) (Fig. 4e).

Author Manuscript Author Manuscript Author Manuscript Author Manuscript

To selectively deplete MDSC in these mice we used agonistic TRAIL-R (DR5) antibody[16–18]. PMN-MDSC in NBM had higher expression of DR5 than neutrophils from AM (Supplementary Fig. 10a). The population of MDSC in lamina propria (LP) was substantially reduced (Supplementary Fig. 10b **and** Fig. 4f). DR5ab significantly (p=0.03) shortened survival (Fig. 4g), increased inflammation score (Fig. 4h), and intestine permeability (Fig. 4i). It caused small but significant (p=0.045) increase in bacterial load in intestine (Fig. 4j) and in blood (Fig. 4k). S100A9KO mice were much more sensitive to NEC induction than WT mice (Supplementary Fig. 10c) indicating the important role of S100A9 in PMN-MDSC protection in NEC.

We next tested the effect of transfer of MDSC from NBM on NEC development. After transfer to mice with NEC, MDSC were readily detectable in intestine (Supplementary Fig. 10d,e). MDSC from NBM caused decrease in inflammation score (Fig. 4l) and intestinal permeability (Fig. 4m). In contrast, Gr-1$^+$ cells from AM did not have effect on gut inflammation (Fig. 4l,m). Injection of AM cells did not affect survival of mice with NEC. In contrast, MDSC from NBM substantially prolonged survival (Fig. 4n). Transfer of MDSC from NBM decreased bacterial load in both intestine and blood. However, no differences between the effect of MDSC and Gr-1$^+$ cells from AM on bacterial load were detected (Fig. 4o).

Thus, it appears that antibacterial effect of MDSC is not a major factor in their effect on NEC. To test this possibility, we used Rag1KO mice lacking T and B cells. Consistent with previous report[19], NEC in Rag1 KO mice had lower inflammation and longer survival than WT mice (Supplementary Fig. 10f–i). However, no differences in bacterial load was evident (Supplementary Fig. 10j,k). Depletion of MDSC in Rag1KO mice (Supplementary Fig. 10l **and** Fig. 4p) did not affect inflammation score (Fig. 4r), intestine permeability (Fig. 4s) or survival of the mice (Fig. 4t). Depletion of MDSC did not affect bacterial load in intestine or circulation in Rag1KO mice (Supplementary Fig. 10m).

We then induced NEC in Rag1-KO mice and performed i.p. transfer of MDSC and CD4$^+$ T cells. Transfer of T cells increased the inflammation (Supplementary Fig. 11a) and intestinal permeability (Supplementary Fig. 11b), which was associated with decrease in survival (Supplementary Fig. 11c). Administration of MDSC abrogated these effects (Supplementary Fig. 11a–c). Despite strong effect of T cell transfer on mouse survival, it did not affect bacterial load. MDSC caused decrease in bacterial load only when mice were transferred with T cells (Supplementary Fig. 11d), which could be due to the decrease in the severity of NEC. Thus, these results indicate that MDSC effect on NEC was mediated via inhibition of T cells.

Induction of NEC was associated with up-regulation of Th17 cells (IL-17A$^+$ and Ror$\gamma$t$^+$) in small intestine. Administration of myeloid cells from AM did not affect that frequency, whereas MDSC from NBM considerably reduced it. MDSC increased the frequency of Foxp3$^+$ Tregs (Supplementary Fig. 11e).

LF treatment of WT mice with NEC caused accumulation of MDSC in LP (Supplementary Fig. 12a). This was associated with decreased intestinal permeability (Supplementary Fig.

Author Manuscript Author Manuscript Author Manuscript Author Manuscript

12b), inflammation (Supplementary Fig. 12c), and prolonged survival (Supplementary Fig. 12d). LF reduced bacterial load both in intestine and circulation (Supplementary Fig. 12e). In sharp contrast, administration of LF to Rag1KO mice did not affect severity of NEC (Supplementary Fig. 12f–h). Administration of T cells enhanced NEC, whereas LF abrogated T-cell induced NEC. Administration of LF had similar antibacterial affect in mice with or without T-cell transfer (Supplementary Fig. 12i). Administration of LF recapitulated the effect of MDSC by down-regulating intestinal Th17 and up-regulating Tregs (Supplementary Fig. 12j).

Thus, in this report, we described the presence of immune suppressive MDSC in healthy mice and humans during the first weeks of life. Most of the cells had the phenotype of PMN-MDSC, which was consistent with the report of increased numbers of granulocytic MDSCs in infants in the first month of life[20]. However, the presence of MDSC was not associated with increased myelopoiesis in NBM since the highest presence of myeloid cells was observed during the first 3 days of life, whereas immune suppressive activity of these cells was observed only after day 4. Granulocytes and monocytes from PM lacked suppressive activity. Our data suggests that LF in mother's milk could be responsible for acquisition of suppressive phenotype by MDSC. Suppressive activity of M-MDSC was mediated by LF induced NO production, whereas PMN-MDSC suppress with mechanism involved S100A9 mediated up-regulation of PGE2. It was consistent with the report that in humans, LF in the presence of GM-CSF could up-regulate S100A9 production[21]. S100A9/A8 proteins were previously implicated in regulation of MDSC expansion[22–24]. However, their role in MDSC mediated suppression was not clear. S100A8 and S100A9 in human neutrophils are arachidonic acid (AA) binding proteins, serving as intermediate intracellular reservoir for AA, thus modulating the activities of AA metabolizing enzymes. Higher AA concentration favors PGE2 production over leukotriene in neutrophils. This process is mediated by the phospholipase A2 (cPLA2) involved in the COX2 mediated generation of PGE2 via microsomal Ptges[25]. Our experiments with S100A9/A8 knockout mice demonstrated that *ptges* expression and PGE2 production is downstream from S100A9/A8. PGE2 can directly inhibit proliferation of T cells via upregulation of cAMP[26]. Apparently, LF effect is cell type dependent, since previous reports demonstrated that LF can negatively regulate PGE2 production in amniotic fluid, enterocytes, and chondrocytes[27–29]. However, these cells lack S100A9/A8 proteins.

We suggest that the presence of MDSC in newborns may represent one of the mechanisms controlling inflammatory response during microbial colonization of gut and lungs in neonates. Our data demonstrate the role of MDSC under steady state conditions and provide a mechanism of their generation, apparently distinct from that utilized in cancer. Our results suggest that MDSC could be utilized as potential therapeutic option in treatment of infants with NEC.

## Online Methods

### Human subjects

Between September 2016 and October 2017, placental cord blood was collected from women during delivery in the Third Affiliated Hospital of Sun Yat-sen University, and

Author Manuscript Author Manuscript Author Manuscript Author Manuscript

Guangzhou Women and Children's Medical Center, Guangzhou, China. The peripheral blood was collected from infants (aged day 0 to 10) delivered in the Third Affiliated Hospital of Sun Yat-sen University (Guangzhou, China) and CHOP in Philadelphia. All subjects were screened for serum HIV antibody, hepatitis B surface antigen (HBsAg), hepatitis C virus (HCV) antibody, hepatitis D virus (HDV) antigen, and HDV antibody and positive individuals were excluded from the study. Women with acute infections (including pneumonia, urinary tract infection) and those with fever were also excluded. Infants presented pathologic jaundice, fever, asphyxia neonatorum and other acute diseases within 7 days after delivery were excluded. Infants born with 2500g–4000g were defined as normal weight (NW), lower than 1500g were considered to be of very low weight (VLW). This study was approved by the Clinical Ethics Review Board of the Third Affiliated Hospital of Sun Yat-sen University, Guangzhou Women and Children's Medical Center, and CHOP hospital. Written informed consent was obtained from all the participants or their legal guardians at the time of admission.

## Flow cytometric analysis of human samples

Peripheral blood mononuclear cell (PBMC) and Cord blood mononuclear cells (CBMC) were isolated from cord blood by Ficoll centrifugation and analyzed within 6 hours after collection. The antibodies used in this study are listed in Table S1. The cell phenotype was evaluatedon a LSRII flow cytometer (BD Bioscience), and data were analyzed with the FlowJo V10.0.7 (FlowJo, OR, USA). Data were acquired as the fraction of labeled cells within a live-cell gate set for minimum 50,000 events. For the flow cytometric sorting, a BD FACSAria cell sorter (BD Bioscience) was used. The strategy for MDSC sorting was $CD14^{-}CD11b^{+}CD15^{+}$ for PMN-MDSC and $CD11b^{+}CD14^{+}HLA\text{-}DR^{-/low}CD15^{-}$ for M-MDSC. Examples of gating are provided in Supplementary Fig. 13.

## Reagents

Reagents used in the study are listed in Table S2.

## Mice

Experiments performed in Sun Yat-sen University (SYSU) were approved by the Institutional Animal Care and Use Committee of Sun Yat-sen University. Experiments performed at Wistar Institute (WI) were approved by IACUC of the Wistar Institute. For experiments in SYSU, C57BL/6 and BALB/c mice were purchased from the Laboratory Animal Center of Sun Yat-sen University and OT-1 transgenic mice were kindly provided by Dr. Hui Zhang (Sun Yat-sen University). Cox-2 KO mice were kindly provide by Dr. Ying Yu (Tianjin Medical University). For experiments at WI, C57BL/6 and BALB/c mice were purchased from Taconic, OT-1 mice from Jackson Lab, S100A9 KO mice were originally provided by Dr. J. Roth (University of Munster), Cox-2 KO mice were obtained from Jackson Lab, LF KO mice were kindly provided by Dr. Grey-Owen (University of Toronto). All mice were bred in pathogen-free facilities, and age-matched littermates were used as controls.

Author Manuscript Author Manuscript Author Manuscript Author Manuscript

### Analysis of MDSCs

Mouse bone marrow cells were harvested by femoral bones flushing and filtered through 80 um pore size cell strainer (Corning, NY, USA). Spleens were mechanically dissociated and filtered. BM cells were cultured in RPMI 1640 medium supplemented with 10% FBS, 20 ng/ml GM-CSF, 20 ng/ml IL-6, and 50 μM 2-ME. The cultures were maintained at 37°C in 5% $CO_2$ -humidified atmosphere in 24-well plates. Medium were refreshed on day 3. Cells were analyzed by flow cytometry on day 6. For flow cytometry, red blood cells were lysed in ACK buffer and cells were stained with different antibodies: CD11b (BV421, BD), Ly6C (PeCy7, BD), Ly6G (FITC, BD) and aqua live dead (Life Technologies). Examples of gating are provided in Supplementary Fig. 13. For PMN-MDSC isolation, cells were labelled with biotinylated Ly6G antibody (Miltenyi) followed by Streptavidin Microbeads (Miltenyi) and separation on MACS Columns (Miltenyi). Two passages on columns were done to maximize cell purity. For M-MDSC isolation, $CD11b^{+}Ly6C^{high}Ly6G^{-}$ cells were sorted on MoFlo®AStrios™ (Becmak Coulter, Brea, CA, USA). All antibodies were obtained from BD Pharmingen. Cell Aqua live dead (Life Technologies) was used to exclude dead cells. For S100A9 intracellular staining, cells were fixed and permeabilized with CytoFix/CytoPerm solution (BD) according to manufacturer's instructions and S100A9 Ab (A647, BD) was used at 1:200 dilution. ROS was evaluated using DCFDA (Abcam, Cambridge, UK) staining.

### MDSC suppression assay

PMN-MDSC were plated in U-bottom 96-well plate (3 replicates) in RMPI with 10% FBS and co-cultured at different ratios with splenocytes from Pmel or OT-1 transgenic mice in the presence of cognate peptides: OT-1 – SIINFEKL, Pmel – EGSRNQDWL. Cells were incubated for 48hr and then [$^{3}$H]-Thymidine (PerkinElmer, Memphis, TN, USA) was added (1μl/well) followed by overnight incubation and counted on TopCount NXT (PerkinElmer). To evaluate M-MDSC suppressive activity, sorted $CD3^{+}$ T cells from spleen were labeled with CFSE (2 μM) (Invitrogen), stimulated with anti- CD3 (5 μg/mL) coated plates and soluble anti- CD28 (1 μg/mL) antibody (eBioscience) and cultured alone or with M-MDSC at different ratios for 3 days. Cells were then stained with CD4-PE-Cy5 and CD8a-PE antibodies, and T-cell proliferation was analyzed by flow cytometry.

### RNA-sequencing data analysis

PMN-MDSC and M-MDSC from spleens of neonates (7 day old) and adult mice (6–8 weeks old) were enriched by CD11b-beads and then sorted on FACSAria cell sorter (BD Bioscience) using $CD11b^{+}Ly6C^{int}Ly6G^{+}$phenotype for PMN-MDSCs and $CD11b^{+}Ly6C^{high}Ly6G^{-}$ for M-MDSCs. The sorting purity was >95%. RNA sequencing was performed using Illumina Hiseq 2500 platform (Illumina, San Diego, CA, USA). VAHTS Total RNA-Seq Library Preparation Kit (Vazyme Biotech Co., Ltd, China) was used for library preparation. Single-end read runs were used, with read lengths up to 50 bp in high output mode, 30M total read counts. Data was aligned using RSEM v1.2.12 software[30] against mm10 genome and gene-level read counts and RPKM values on gene level were estimated for ensemble transcriptome. Samples with at least 80% aligned reads were analyzed. DESeq2[31] was used to estimate significance between any two experimental

Author Manuscript Author Manuscript Author Manuscript Author Manuscript

groups. Overall changes were considered significant if passed FDR<5% thresholds with an additional threshold on fold change (fold>5) taken to generate the final gene set. Gene set enrichment analysis was done using QIAGEN's Ingenuity® Pathway Analysis software (IPA®, QIAGEN Redwood City, www.qiagen.com/ingenuity) based on "Functions", "Canonical Pathways", "Upstream Regulators" and "Networks" options. Gene overlap between microarray and RNA-seq study was done using Entrez IDs and Pearson correlation coefficients were calculated between any pair of samples. Each microarray sample correlation value was then normalized to Pearson correlation versus average RNA-seq profile. RNA-seq data were deposited to GEO data repository (accession number GSE97993).

### Quantitative Real Time PCR (qRT-PCR)

RNA was extracted using Total RNA Kit I (Omega, Biel/Bienne, Switzerland) according to manufacturer's instructions. Primer sequences are listed in Table S3.

### ELISA

Cells were cultured 24hr at $2x10^6$/ml in RPMI with 10% FBS. Supernatants were centrifuged at 300g for 5 min at 4°C and filtered through 0.22 μm filter. PGE2, S100A9 or LF ELISA kits (Invitrogen, Carlsbad, CA, USA) were used to measure the amount of corresponding proteins.

### LF treatment

For *in vivo* experiments, three weeks old WT and S100A9KO mice were treated with LF (Sigma Aldricht, St. Louis, MO, USA) (5 mg/mouse i.p. in PBS (vehicle) daily for 8 days), PBS was used as vehicle control. For *in vitro* treatment, mouse bone marrow (BM) cells or cord blood mononuclear cells from VLW babies were cultured in the presence of GM-CSF and IL-6, in the presence or absence of LF protein (700 μg/ml) for 6 days.

### Allergy-induced airway inflammation mouse model

BALB/C mice at different age were intraperitoneally sensitized with 5 μg/g OVA (Grade V, Sigma-Aldrich) emulsified in 200 μg/g of aluminum hydroxide (ThermoImject® Alum) on days 0 and 7, followed by intranasal challenge with OVA (5 μg/μl of PBS) once on day 17 to 21. One day after the last challenge, mice were sacrificed and lung inflammation was examined [32]. For MDSC transfer experiments, 3 million of adult spleen neutrophils, neonatal spleen PMN-MDSC, neonatal spleen M-MDSC and vehicle control (PBS) was given i.v. 1 day before each sensitization.

### Necrotizing Enterocolitis (NEC) induction

NEC induction was performed as described[33]. Briefly, neonates were taken from the parents and were fed with formula (Esbilac, PetAg, Hampshire, IL, USA) via oral gavage (100–200 μl, 3–4 times/day) during the observation time. On day 0 mice were gavaged with bacteria obtained from fecal suspension of adult healthy mice caecum at $7x10^7$ CFU/mouse. Starting from day 1, mice were subjected to hypoxia-cold shock cycle twice a day for three days. Mice were put in hypoxia chamber at 1% $O_2$ for 2min and then immediately transferred to

Author Manuscript Author Manuscript Author Manuscript Author Manuscript

an ice slurry in a pre-cold bucket for 10min. After shock, mice were put back in the cage and observed for NEC symptoms, including severe abdominal distension, apnea, cyanosis, and lethargy. Small intestines were collected and fixed in 10% buffered formalin for histological examination. Fluorescein isothiocyanate (FITC) labeled dextran (FD7000, molecular weight 73,000) (Sigma-Aldrich Inc., St. Louis, MO) was used to assess mucosal permeability as described previously[34].

In MDSC depletion experiment, 40 μg/g of anti-DR5 (BioXcell) were given to 6 day neonates i.p. 1 hour before and 36hr after initiation of NEC procedure, Rat IgG Isotype was used as control. To induce NEC in KO mice, 6 days old mice (WT, S100a9KO, or Rag1-KO) were used. In MDSC transfer experiment, 1 million neonatal spleen Gr-1+ cells were given i.p. per mice 1 hour before initial of NEC procedure, adult mice spleen Gr-1+ cells and vehicle (PBS) were used as control. For T cell transfer in Rag1-KO, $4x10^6$ spleen $CD4^+$ T cells from NEC mice were used. In the LF treatment group, LF (0.25g/kg in PBS) was given to 1 day neonates by i.p. injection daily 1 hour before NEC procedure, till the end of experiment.

### qPCR measurement of bacterial loading

DNA were extracted from serum and intestine, the total amount of bacterial sRNA was then quantified with bacteria-specific 16S primers, as described previously[70].

### Cross-Fostering

Breeding pairs of WT and LFKO mice were concurrently set up when adult were 5–6 weeks old. Only litters born on the same day were enrolled in the cross-fostering experiments. After delivery, WT adult female was removed from her cage and put with the LFKO litter and vice versa. Fostered pups were maintained until day 7 after birth, then sacrificed for functional tests.

### Statistics

In most experiments, statistical analyses were done using two-tailed unpaired Student's t tests. Where indicated non-parametric Mann-Whitney tests were used. Survival curves were compared using the Log-rank (Mantel-Cox) test and Gehan-Breslow-Wilcoxon tests. Statistical tests were performed using GraphPad Prism version 7.0 and SPSS Statistics 20.0. P values of 0.05 were considered significant. RNAseq data were analyzed by RSEM v1.2.12 software, DESeq2, Ingenuity® Pathway Analysis software.

### Data availability statement

RNAseq data set was deposited to GEO data repository (accession number GSE97993).

## Supplementary Material

Refer to Web version on PubMed Central for supplementary material.

Author Manuscript Author Manuscript Author Manuscript Author Manuscript

## Acknowledgments

This work was supported by Wistar Institute Animal and Bioinformatics core facilities as well as the following grants to DG and VK: NIH grant CA165065. The work was also supported by the Recruitment Program for Foreign Experts (The Thousand Talents Plan, WQ2014440O204), Start-up Fund for High-level Talents of Sun Yat-sen University, The Leading Talents of Guangdong Province Program (DG). This work was supported by the following grants to JZ: Introduction of Innovative R&D Team Program of Guangdong Province (2009010058), Guangdong Province Universities and Colleges Pearl River Scholar Funded Scheme (GDUPS, 2014), National Natural Science Foundation of China (91542112; 81571520, 81771665, 81742002), The Provincial Talents Cultivated by "Thousand-Hundred-Ten" Program of Guangdong Province, 111 Project (B12003). We thank Dr. Grey-Owen (University of Toronto) and Dr. Conneely (Baylor College of Medicine) for providing us with LF KO mice. We thank Dr. Ying Yu (Tianjin Medical University) for providing Cox2 KO mice.

## References

1. Marvel D, Gabrilovich DI. Myeloid-derived suppressor cells in the tumor microenvironment: expect the unexpected. J Clin Invest. 2015; 125:3356–3364. [PubMed: 26168215]
2. Gabrilovich DI. Myeloid-Derived Suppressor Cells. Cancer Immunol Res. 2017; 5:3–8. [PubMed: 28052991]
3. Bronte V, et al. Recommendations for myeloid-derived suppressor cell nomenclature and characterization standards. Nat Commun. 2016; 7:12150. [PubMed: 27381735]
4. Veglia F, Perego M, Gabrilovich D. Myeloid-derived suppressor cells coming of age. Nat Immunol. 2018 in press.
5. Obermajer N, et al. PGE(2)-driven induction and maintenance of cancer-associated myeloid-derived suppressor cells. Immunol Invest. 2012; 41:635–657. [PubMed: 23017139]
6. Nagaraj S, et al. Antigen-specific CD4(+) T cells regulate function of myeloid-derived suppressor cells in cancer via retrograde MHC class II signaling. Cancer Research. 2012; 72:928–938. [PubMed: 22237629]
7. Youn JI, Collazo M, Shalova IN, Biswas SK, Gabrilovich DI. Characterization of the nature of granulocytic myeloid-derived suppressor cells in tumor-bearing mice. J Leukoc Biol. 2012; 91:167–181. [PubMed: 21954284]
8. Manitz MP, et al. Loss of S100A9 (MRP14) results in reduced interleukin-8-induced CD11b surface expression, a polarized microfilament system, and diminished responsiveness to chemoattractants in vitro. Mol Cell Biol. 2003; 23:1034–1043. [PubMed: 12529407]
9. Park JY, Pillinger MH, Abramson SB. Prostaglandin E2 synthesis and secretion: the role of PGE2 synthases. Clin Immunol. 2006; 119:229–240. [PubMed: 16540375]
10. Deshmukh HS, et al. The microbiota regulates neutrophil homeostasis and host resistance to Escherichia coli K1 sepsis in neonatal mice. Nat Med. 2014; 20:524–530. [PubMed: 24747744]
11. Vogel HJ. Lactoferrin, a bird's eye view. Biochemistry and cell biology = Biochimie et biologie cellulaire. 2012; 90:233–244. [PubMed: 22540735]
12. Warner BB, Tarr PI. Necrotizing enterocolitis and preterm infant gut bacteria. Seminars in fetal & neonatal medicine. 2016; 21:394–399. [PubMed: 27343151]
13. Denning TL, Bhatia AM, Kane AF, Patel RM, Denning PL. Pathogenesis of NEC: Role of the innate and adaptive immune response. Seminars in perinatology. 2016
14. Condamine T, et al. Lectin-type oxidized LDL receptor 1 distinguishes population of human polymorphonuclear myeloid-derived suppressor cells in cancer patients. Science Immunol. 2016; 1
15. Niño D, Sodhi C, Hackam D. Necrotizing enterocolitis: new insights into pathogenesis and mechanisms. Nat Rev Gastroneterol Hepatol. 2016; 13:590–600.
16. Condamine T, et al. ER stress regulates myeloid-derived suppressor cell fate through TRAIL-R-mediated apoptosis. J Clin Invest. 2014; 124:2626–2639. [PubMed: 24789911]
17. James BR, et al. CpG-mediated modulation of MDSC contributes to the efficacy of Ad5-TRAIL therapy against renal cell carcinoma. Cancer Immunol Immunother. 2014; 63:1213–1227. [PubMed: 25143233]

Author Manuscript Author Manuscript Author Manuscript Author Manuscript


18. Dominguez GA, et al. Selective Targeting of Myeloid-Derived Suppressor Cells in Cancer Patients Using DS-8273a, an Agonistic TRAIL-R2 Antibody. Clin Cancer Res. 2017; 23:2942–2950. [PubMed: 27965309]
19. Egan CE, et al. Toll-like receptor 4-mediated lymphocyte influx induces neonatal necrotizing enterocolitis. J Clin Invest. 2016; 126:495–508. [PubMed: 26690704]
20. Gervassi A, et al. Myeloid derived suppressor cells are present at high frequency in neonates and suppress in vitro T cell responses. PloS one. 2014; 9:e107816. [PubMed: 25248150]
21. Curran CS, Bertics PJ. Lactoferrin regulates an axis involving CD11b and CD49d integrins and the chemokines MIP-1alpha and MCP-1 in GM-CSF-treated human primary eosinophils. Journal of interferon & cytokine research : the official journal of the International Society for Interferon and Cytokine Research. 2012; 32:450–461.
22. Cheng P, et al. Inhibition of dendritic cell differentiation and accumulation of myeloid-derived suppressor cells in cancer is regulated by S100A9 protein. J Exp Med. 2008; 205:2235–2249. [PubMed: 18809714]
23. Heinemann AS, et al. In neonates S100A8/S100A9 alarmins prevent the expansion of a specific inflammatory monocyte population promoting septic shock. FASEB J. 2017; 31:1153–1164. [PubMed: 27993995]
24. Sinha P, et al. Proinflammatory s100 proteins regulate the accumulation of myeloid-derived suppressor cells. J Immunol. 2008; 181:4666–4675. [PubMed: 18802069]
25. St-Onge M, et al. Characterization of prostaglandin E2 generation through the cyclooxygenase (COX)-2 pathway in human neutrophils. Biochim Biophys Acta. 2007; 1771:1235–1245. [PubMed: 17643350]
26. Wehbi VL, Tasken K. Molecular Mechanisms for cAMP-Mediated Immunoregulation in T cells - Role of Anchored Protein Kinase A Signaling Units. Frontiers in immunology. 2016; 7:222. [PubMed: 27375620]
27. Talukder JR, Griffin A, Jaima A, Boyd B, Wright J. Lactoferrin ameliorates prostaglandin E2-mediated inhibition of Na+-glucose cotransport in enterocytes. Canadian journal of physiology and pharmacology. 2014; 92:9–20. [PubMed: 24383868]
28. Trentini A, et al. Vaginal Lactoferrin Modulates PGE2, MMP-9, MMP-2, and TIMP-1 Amniotic Fluid Concentrations. Mediators of inflammation. 2016; 2016:3648719. [PubMed: 27872513]
29. Rasheed N, Alghasham A, Rasheed Z. Lactoferrin from Camelus dromedarius Inhibits Nuclear Transcription Factor-kappa B Activation, Cyclooxygenase-2 Expression and Prostaglandin E2 Production in Stimulated Human Chondrocytes. Pharmacognosy research. 2016; 8:135–141. [PubMed: 27034605]
30. Li B, Dewey CN. RSEM: accurate transcript quantification from RNA-Seq data with or without a reference genome. BMC bioinformatics. 2011; 12:323. [PubMed: 21816040]
31. Love MI, Huber W, Anders S. Moderated estimation of fold change and dispersion for RNA-seq data with DESeq2. Genome biology. 2014; 15:550. [PubMed: 25516281]
32. Mosconi E, et al. Breast milk immune complexes are potent inducers of oral tolerance in neonates and prevent asthma development. Mucosal immunology. 2010; 3:461–474. [PubMed: 20485331]
33. Tian R, et al. Characterization of a necrotizing enterocolitis model in newborn mice. International journal of clinical and experimental medicine. 2010; 3:293–302. [PubMed: 21072263]
34. Rager TM, Olson JK, Zhou Y, Wang Y, Besner GE. Exosomes secreted from bone marrow-derived mesenchymal stem cells protect the intestines from experimental necrotizing enterocolitis. Journal of pediatric surgery. 2016; 51:942–947. [PubMed: 27015901]

Author Manuscript Author Manuscript Author Manuscript Author Manuscript

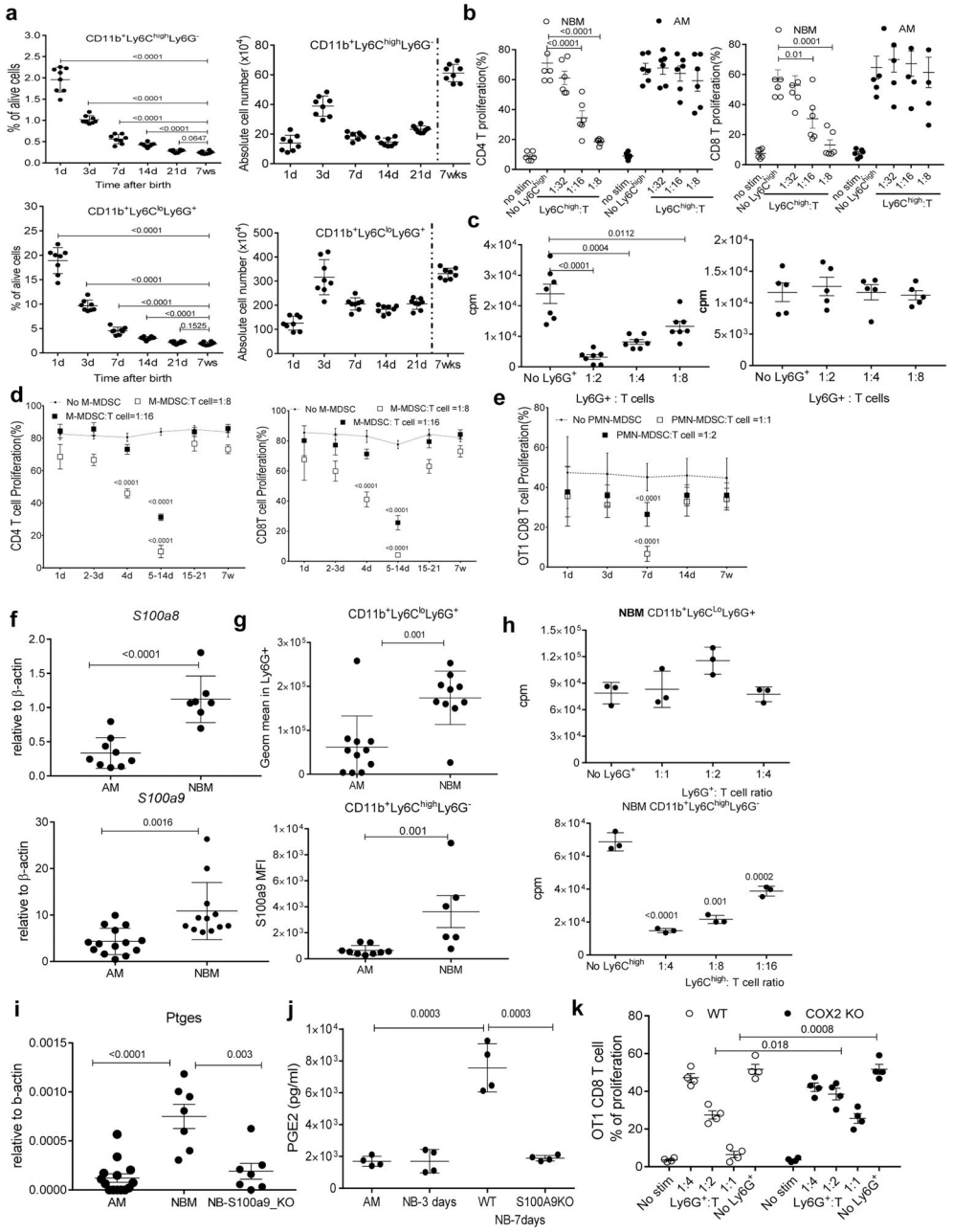


**Figure 1. Expansion of MDSC in newborn mice**

**a**. The proportion and absolute number of the populations of splenocytes at different time after birth (n=8). In AM the total number of splenic cells could not be directly compared with that in NBM due to the much larger spleen size. These results are provided for reference only. **b.** CD3/CD28 inducible proliferation of $CD4^+$ and $CD8^+$ T cells in the presence of M-MDSC isolated from newborn (NBM) and adult (AM) mice. No stim - not activated T cells (negative control); No MDSC - T cell proliferation in the absence of MDSC. Proliferation was measure by CFSE dilution. (n=4–6). **c**. Antigen-specific proliferation of $CD8^+$ T cells in the presence of PMN-MDSC isolated from NBM and AM.

Author Manuscript Author Manuscript Author Manuscript Author Manuscript

Proliferation was measure in triplicates by $^{3}$H-thymidine uptake. OT-1 T cells were used as responders in antigen-specific suppression assay (cpm =counts per minute). Experiments were performed in triplicates. Individual experiments are shown. Left panel NBM (n=7), right panel AM (n=5). **d**. Antigen non-specific suppression assays of M-MDSC isolated from NB spleen at different time points after birth (n=4) **e**. Antigen-specific suppression assays of PMN-MDSC isolated from NB spleen at different time points after birth. (n=4). In all plots mean ± SD are shown. **f**. *s100a8* and *s100a9* gene expression in PMN-MDSC from 7-day NBM and AM mice (n=7–14). **g**. Intracellular S100A9 protein expression measured by flow cytometry in PMN-MDSC or M-MDSC from 7-day NBM or AM mice. Please note the differences in the scale of MFI between PMN-MDSC and M-MDSC (n=6–11). **h**. Antigen specific suppression assays of PMN-MDSC and M-MDSC isolated from spleens of 7-day old S100A9 KO mice. Cell proliferation was measured in triplicates by $^{3}$[H]-thymidine uptake. Typical example of three experiments is shown. **i.** *Ptges* gene expression in PMN-MDSC (qRT-PCR). NBM (n=7), NB S100A9 KO (n=7), AM control (n=14). **j**. Amount of PGE2 measured by ELISA in cell supernatants from 24hr culture of PMN-MDSC from adult and NB (3 or 7 days old) WT mice or S100a9 KO 7 days old NB mice (n=4). **k**. Antigen specific suppression assay of PMN-MDSC isolated from spleens of 7 day-old NB WT and Cox2 KO mice (n=4). In all plots mean ± SD are shown. In most panels p values are shown on the graphs.

Author Manuscript Author Manuscript Author Manuscript Author Manuscript

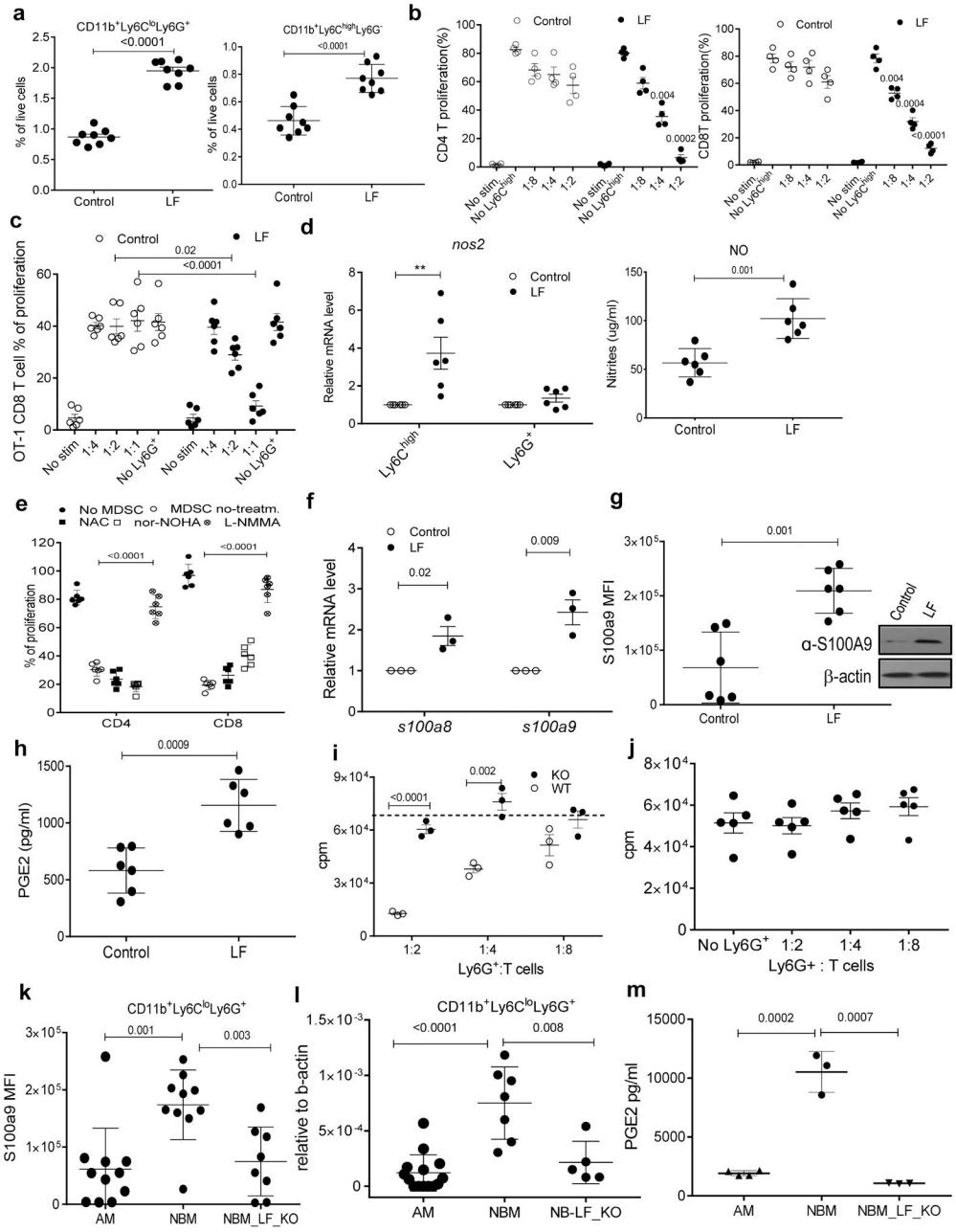


**Figure 2. Lactoferrin is responsible of accumulation of MDSC in newborn mice**

**a.** Proportion of monocytes and neutrophils in LF treated 3 weeks old mice (n=8). Control – mice treated with PBS. **b**. Suppression of CD3/CD28 stimulated T cells by M-MDSC isolated from AM treated with LF or PBS (control) (n=4) **c.** Antigen-specific suppression assay of PMN-MDSC isolated from AM treated with LF (n=6). **d.** Expression of *nos2* in MDSC from LF treated mice (n=6) (left panel). Amount of NO in M-MDSC from LF treated mice (n=6) (right panel). **e.** Suppression of CD3/CD28 stimulated T cells by M-MDSC from LF-treated mice in the presence of inhibitors of ROS (NAC), arginase-I (nor-NOHA), or Nos2 (L-NMMA) (n=6). **f**. Expression of *s100a9* and *s100a8* genes in PMN-

Author Manuscript Author Manuscript Author Manuscript Author Manuscript

MDSC from LF treated mice (n=3). **g**. Mean fluorescence intensity (MFI) of intracellular expression of S100A9 protein detected by flow cytometry in PMN-MDSC from AM treated with LF (n=6); Inset – amount of S100A9 protein detected by Western Blot. Representative result of three independent experiments is shown. **h**. PGE2 amount in cell lysates from 24hr culture of PMN-MDSC isolated from AM treated with LF (n=6). **i.** Antigen-specific T cell suppressive activity of PMN-MDSC isolated from LF treated wild-type and S100A9 KO mice. Proliferation was measure by $^{3}$[H]-thymidine uptake in triplicates. Typical example of three performed experiments is shown. Dotted line – the level of T cell proliferation in the absence of MDSC. **j.** Antigen specific suppression assays of PMN-MDSC isolated from LF KO mice. Experiment was performed in triplicates. Results of 5 experimtnts are shown. **k.** Mean fluorescence intensity (MFI) of intracellular S100A9 protein expression in PMN-MDSC in AM (n=11),NB WT (n=10), and LFKO (n=8) mice. **l.** Expression of *ptges* in PMN-MDSC from AM (n=13), NB WT (n=7), and LF-KO (n=5) mice. **m.** Amount of PGE2 measured by ELISA in cell lysates from 24hr culture of PMN-MDSC from AM (n=4) and NBM WT mice (n=2) or LF KO NBM (n=2). In all plots mean ±SEM are shown. P values in two-tailed Student's test are shown on the graphs.

Author Manuscript Author Manuscript Author Manuscript Author Manuscript

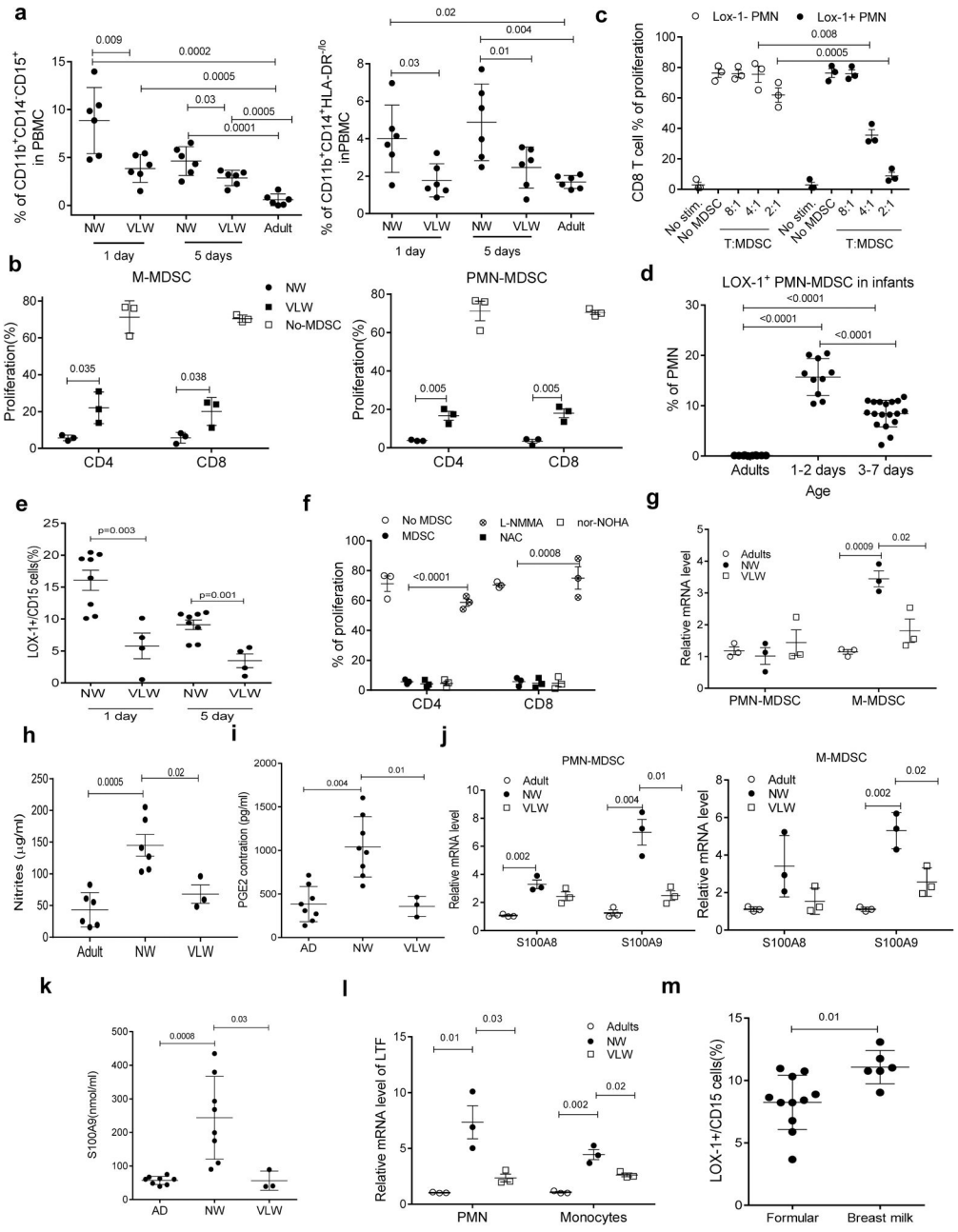


**Figure 3. MDSC in human infants**

**a**. Proportion of MDSC in peripheral blood of infants. PMN-MDSC (left panel) and M-MDSC (right panels) were evaluated in PBMC of peripheral blood of infants with normal (NW) and very low weight (VLW) at indicated time after birth (n=6). Individual data and SD are shown. **b.** Functional activity of MDSC from infants. M-MDSC and PMN-MDSC were sorted from PBMC of infants with normal weight (NW) and very low weight (VLW) and added to T cells isolated from blood and stimulated with CD3/CD28 antibody. Proliferation was measured in triplicates using CFSE labeling (n=3). **c–e.** LOX-1$^{+}$ PMN-MDSC in newborns. **c.** LOX-1$^{+}$ and LOX-1$^{-}$ CD15$^{+}$ cells were isolated from peripheral blood of

Author Manuscript Author Manuscript Author Manuscript Author Manuscript

newborn infants and tested in suppressive activity against CD3/CD28 stimulated T cells. Proliferation was measured in triplicates using CFSE staining (n=3). **d.** Proportion of LOX-1$^+$ cells among CD15$^+$ neutrophils in infants of different age, 1–2 days (n=10), 3–7 days (n=18), adults (n=7). Individual results and SD are shown. **e.** Proportion of LOX-1$^+$ cells in NW (n=8) and VLW (n=4) infants of different age. Individual results are shown. **f–l.** Mechanisms regulating MDSC activity in infants. Samples of blood were collected from newborn infants 1–5 days after birth. M-MDSC and PMN-MDSC were sorted from PBMC. **f.** Suppressive activity of M-MDSC from NW infants in the presence of inhibitors of ROS (NAC), arginase I (nor-NOHA) or NOS2 (L-NMMA). Effectors were CD4$^+$ or CD8$^+$ T cells stimulated with CD3/CD28 antibodies. Proliferation was measured in triplicates using CFSE staining (n=3). **g.** Expression of *NOS2* in M-MDSC (n=3). **h.** Nitrites produced by M-MDSC. NW (n=6), VLW (n=3), control cells from adults (n=6). Individual results, meant and SD are shown. **i.** The amount of PGE2 produced by PMN-MDSC and measured by ELISA in cells lysates. NW and adults - n=8, VLW - n=3. Individual results, mean and SD are shown. **j.** Expression of *S100A8* and *S100A9* in PMN-MDSC and M-MDSC measured by qPCR (n=3). **k.** The amount of S100A9 protein in cell lysates of PMN-MDSC. NW - n=8, VLW - n=3 adults - n=8. **l.** Expression of *LTF* in PMN-MDSC and M-MDSC (n=3). **m.** LOX-1$^+$ PMN-MDSC in blood of 5 days old infants received formula (n=11) or mother's milk (n=6). In all panels, mean and SD are shown. P values in two-tailed Student's test are shown on the graphs.

Author Manuscript
Author Manuscript
Author Manuscript
Author Manuscript



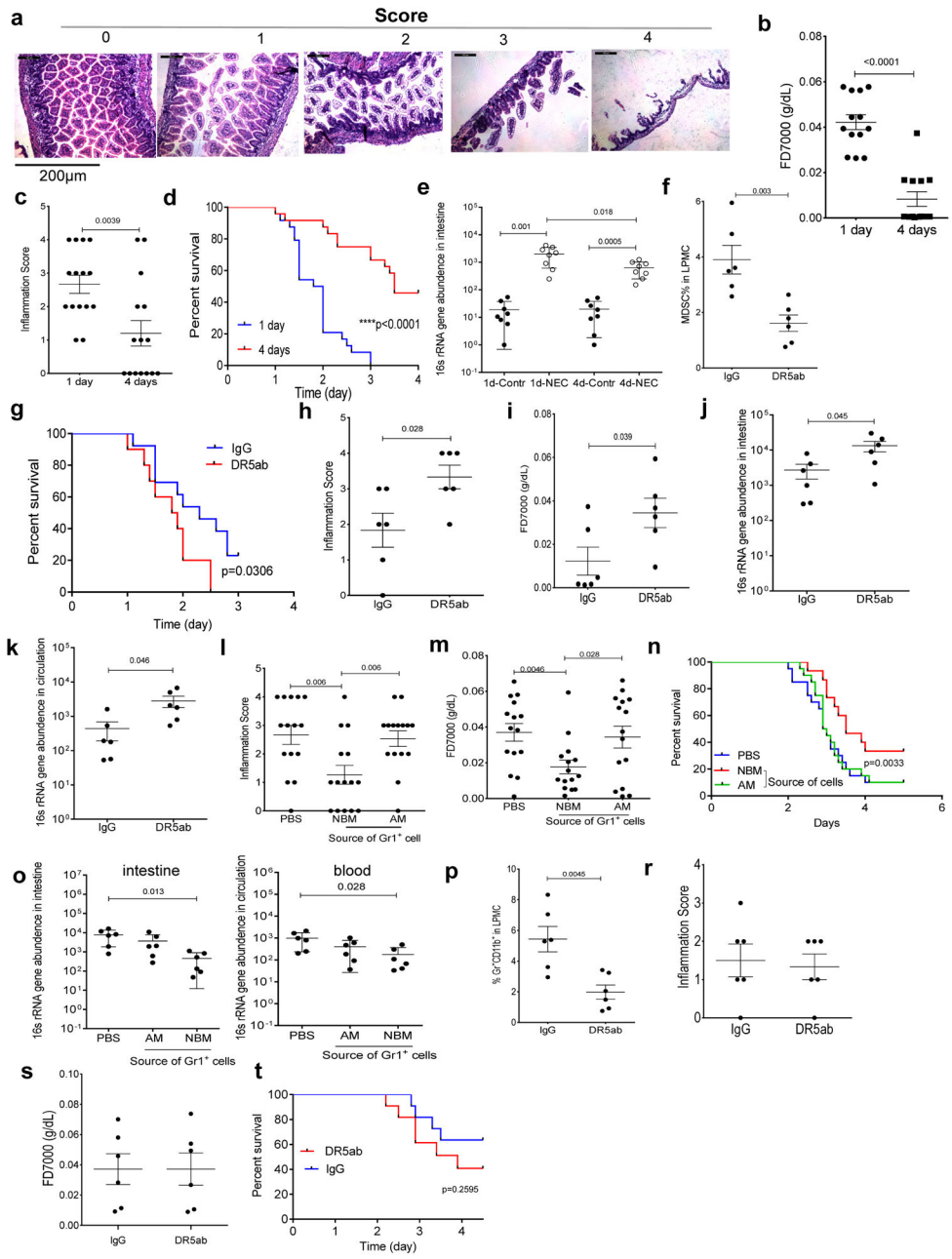


**Figure 4. MDSC role in Necrotizing Enterocolitis (NEC) experimental model**

**a.** Representative images of mice intestine after NEC induction. Numbers in the pictures represent NEC severity from 0 (normal epithelium) to IV (most severe NEC). **b**. Detection of FD7000 (directly proportional to intestine permeability) (n=13), **c**. small intestine inflammation score (n=15), **d.** survival (n=24) in one day and four days old mice after NEC induction. **e.** Bacterial load in small intestine of mice evaluated using 16s rRNA gene abundance analysis (n=8); **f**. Flow cytometry analysis of MDSC presence in lamina propria (LP) after MDSC depletion with DR5 antibody (n=6). **g**. Survival analysis of WT NEC mice with MDSC depletion by DR5ab (n=13) or treated with IgG (n=10). **h**. Small intestine

Author Manuscript Author Manuscript Author Manuscript Author Manuscript

inflammation score in 4 days old mice after MDSC depletion (n=6). **i**. FD7000 after MDSC depletion (n=6). **j,k.** Bacterial load was evaluated in intestine (n=6) **(j)** and blood (n=6) **(k)**. Bacterial load was normalized to the level in NBM without NEC. Values for individual mice are shown. **l**. Inflammation score in small intestine of NBM after treatment with exogenous $Gr1^+$ cells from NBM, adult mice (AM) or vehicle control (PBS) (n=15). **m**. intestine permeability (n=15); **n**. Survival of mice after NEC induction and treatment with $Gr1^+$ cells from NBM (n=20), AM (n=15) or vehicle control (PBS) (n=15). **o**. Bacterial load was evaluated in intestine and blood (n=6). **p**. Flow cytometry analysis of MDSC presence in lamina propria (LP) of Rag1KO mice with induced NEC treated with DR5 antibody or control IgG (n=6). **r**. Small intestine inflammation score of Rag1KO mice with induced NEC treated with DR5 antibody (n=6) **s**. FD7000 in mice treated with DR5 antibody (n=6). **t**. Survival analysis of mice treated with DR5 antibody or IgG after NEC induction (n=11). Individual values and SD are presented. Results of individual mice are shown. In all panels, mean and SD are shown. P values in two-tailed Student's test are shown on the graphs.